Journal of Arid Environments 122 (2015) 46–58

Contents lists available at ScienceDirect

Journal of Arid Environments

journal homepage: www.elsevier.com/locate/jaridenv

Groundwater management options in an arid environment: The Nubian Sandstone Aquifer System, Eastern Sahara

Ahmed Sefelnasr [a, *], Wolfgang Gossel [b], Peter Wycisk [b]

[a] Geology Department, Faculty of Science, Assiut University, 71516 Assiut, Egypt
[b] Institute of Geosciences, Martin Luther University, V.-Seckendorff Platz 3, 06120 Halle, Germany

ARTICLE INFO

Article history:
Received 21 July 2013
Received in revised form
21 May 2015
Accepted 15 June 2015
Available online xxx

Keywords:
Western Desert
Groundwater resources
Scenarios
GIS
Transboundary Aquifer

ABSTRACT

Groundwater is the only water resource across the "hyper" arid Eastern Sahara. Management of this resource is imperative for the sustainable development approaches. A 3D GIS-based groundwater flow model for the Nubian Sandstone Aquifer System (NSAS) was developed to simulate the groundwater management options for the different development areas/oases within the aquifer, and to predict the environmental impact of the present and future groundwater extraction schemes on the whole system. Based on the actual and planned extraction rates of the NSAS, five extraction scenarios were suggested to investigate the most feasible groundwater management option in terms of the economic lifting depth until year 2100. The model was calibrated and validated under the transient conditions. The calibrated model was then used for the prediction simulations. The results of simulating the present extraction rates of the NSAS until 2100 showed that the free flowing phenomenon will disappear all over the modeled area. At this simulation time, a groundwater volume of 354 km^3 will be extracted from the aquifer storage. Scenario 3 was found to be the optimal groundwater management option that meets the development ambitions and at the same time keeps the safe economic lifting depth as well.

1. Introduction

The area of the Nubian Sandstone Aquifer System (Fig. 1) is composed of one huge, unbroken tract of true desert area which is characterized by extreme aridity and rainfall scarcity. The only slight exceptions are the narrow littoral zone extending along the Mediterranean Sea and the most southern margins of the area that receive scanty amounts of rainfall. Islands of life in the interior of this desert are represented by the oases regions, which are located in a series of depressions in the desert plateau and owe their existence exclusively to the groundwater resources (Williams and Faure, 1980; White, 1983; Cloudsley-Thompson, 1984).

The climate of the Sahara has undergone noticeable variations between wet and dry over the last few tens of thousands of years. The groundwater within the NSAS aquifer is very old, however, the last wet period occurred 4000–8000 years BP as discussed by many authors (Pachur et al., 1987; Heinl and Brinkmann, 1989; Pachur et al., 1990; Pachur, 1999; Kröpelin, 1999; El-Baz et al., 2000; Kröpelin, 2001; Sadek et al., 2001; Thorweihe and Heinl, 2002; Sturchio et al., 2004; Gossel et al., 2006, 2010b; Voss and Soliman, 2014).

As stated in several modern publications (i.e. CEDARE, 2001, 2002; Ebraheem et al., 2002, Ebraheem, 2003; Ebraheem et al., 2003, 2004; Ghoneim and El-Baz, 2007; Gossel et al., 2004, 2006, 2008; Sefelnasr, 2002, 2007, 2008; Sefelnasr et al., 2006a,b; Sefelnasr et al., 2014; Voss and Soliman, 2014) the water of the (shared) Nubian Sandstone Aquifer is non-renewable and shared among Egypt, Libya, Sudan, and Chad (Fig. 1). Most of the present water extracted from the NSAS is used for agriculture, either for large development projects in Libya or for farms located in old traditional oases in Egypt (New Valley). The area occupied by the aquifer system is about 2.35 million km^2.

The aquifer is of significant importance because it is the only water resource for this arid area. The increasing demographic growth and the lack of renewable fresh water resources in this arid region have resulted in an increasing attention to the groundwater potential represented by the NSAS. Many attempts were made by Egypt and Libya to develop and utilize this aquifer system during the last three decades, this in turn affects directly the groundwater resources of the aquifer and results in developing huge drawdown depressions around the well fields in the corresponding areas.

* Corresponding author.
E-mail address: ahmed.sefelnasr@science.au.edu.eg (A. Sefelnasr).

http://dx.doi.org/10.1016/j.jaridenv.2015.06.009
0140-1963/

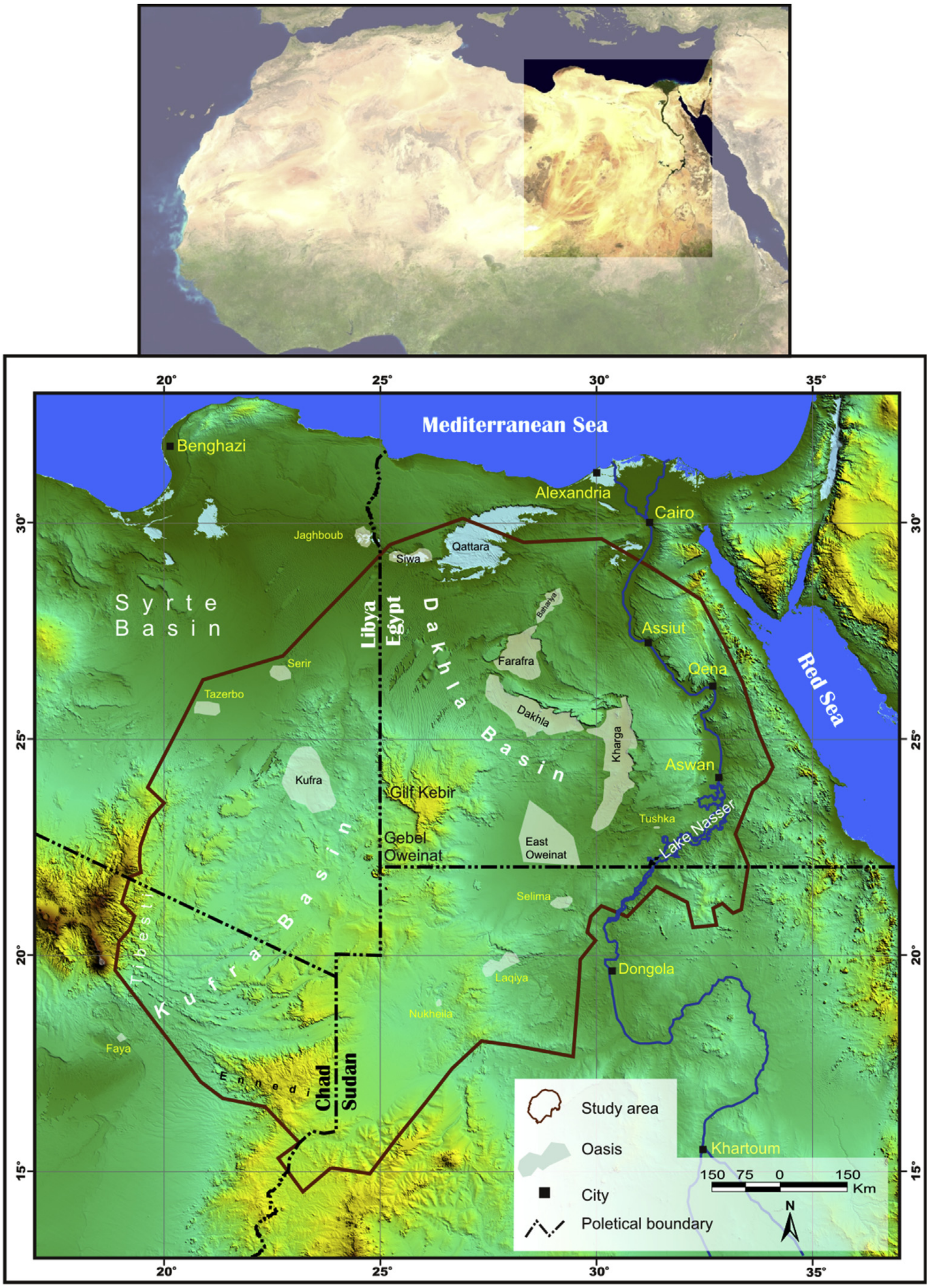

Fig. 1. A DEM of the Eastern Sahara including the study area of the Nubian Sandstone Aquifer System and the development areas. Sources: USGS (2004) and NASA (2005, 2006).

Through the aridity and the non-renewability of the area, the groundwater exploitation from the NSAS has to be managed on basis of groundwater demand, availability and socio-economic aspects. This work is an attempt to simulate different groundwater management schemes based on the given groundwater extraction values for both actual and planned extraction rates.

The data framework for NSAS composed of large aggregations of spatial datasets and records in assorted formats. The powerful tools of ArcGIS were utilized to construct and develop a coherent Geodatabase for the NSAS that allowed for compiling those datasets in a unique structure and defining the topological and temporal relationships. Working with and leveraging the capabilities of the Geodatabase platform made it easier to accomplish the relevant spatial analysis and manipulation, prepare the data as an input for different modeling systems as well as to update the data.

Geodatabase is used and incorporated to establish a conceptual framework to model the real hydrogeologic system, which is an essential step before the development of a numerical groundwater flow model. This includes different assumptions which lead to the estimation or quantification of the different components of the aquifer system, including hydraulic conductivities, storativities, etc. The period 1960–2005 was chosen as a calibration period based on the availability and temporal distribution of the data. Different steps were carried out to simulate the different groundwater management options for the system, among them:

1. Construction and development of a coherent Geodatabase to facilitate the storing, interpolation, manipulation, analyzing, validation and spatial control of the data.
2. Development of a 3D-regional groundwater flow model for the NSAS.
3. Calibration of the regional groundwater flow model against predefined criteria using numerical simulation techniques.
4. The calibrated model is further used to determine the impact of the present and planned extraction rates on the aquifer behavior by making the necessary prediction-simulations to accomplish a good management scheme for the NSAS.

2. Physical, geological, and hydrogeological setting

The sediments body of the study area forms huge morphologic depression structure in the areas of Chad and Libya, as the sediments outcrop at all margins of the basin and the older sediments are generally overlain by the younger ones in the direction of the depression center (Knetsch and Yallouze, 1955; Ibrahim, 1956). In North Sudan and Egypt, a vast monoclinal structure occurs where the older formations outcrop at the southern localities, whereas they generally dip, increase in thickness, and disappear under the younger formations northward as shown in Fig. 2 (Himida, 1970; Hermina, 1990).

Moving from the southern localities of the area northward, the

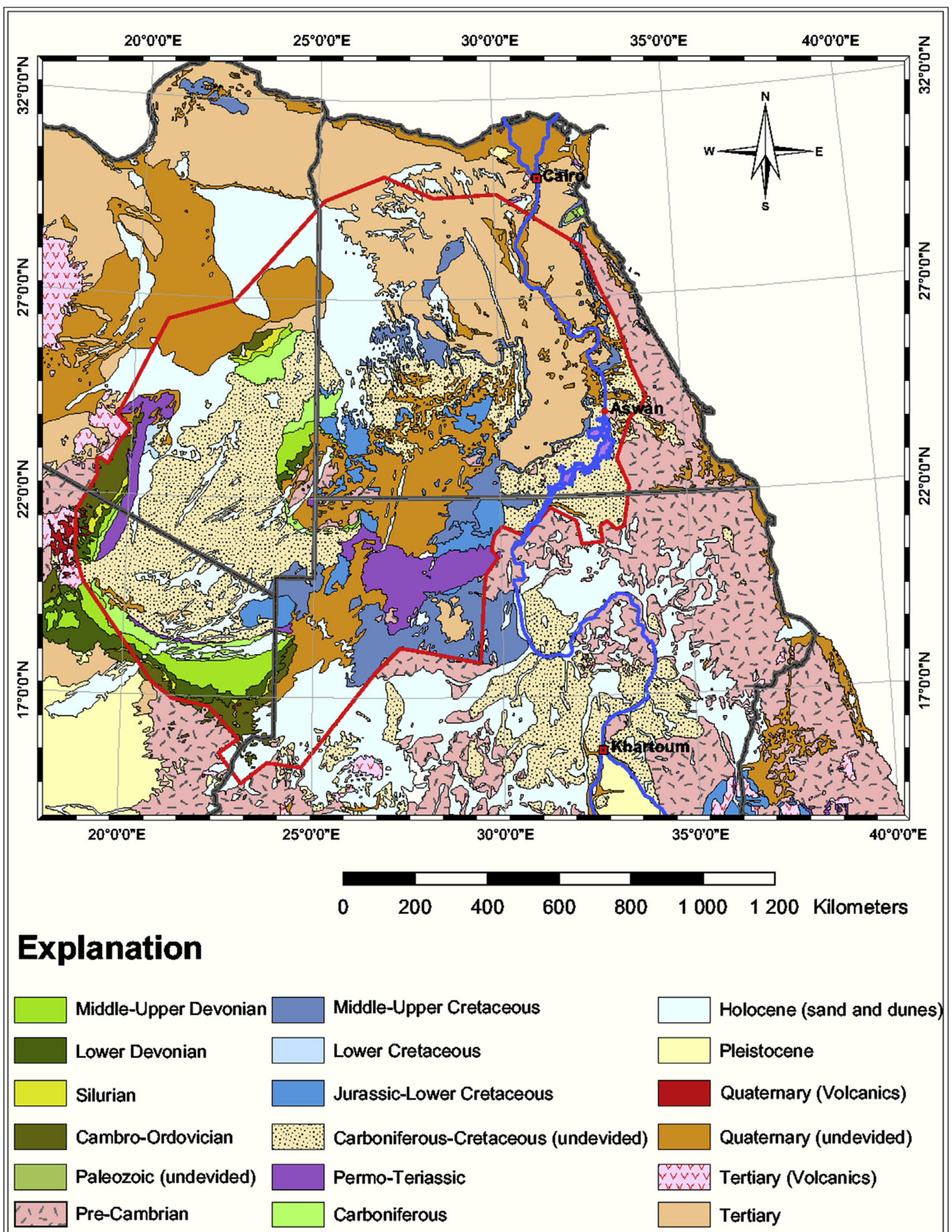

Fig. 2. Geological map of the NSAS. Digitized from maps of CONOCO (1987) and USGS (2004).

rocks of the basement complex are gradually overlain by a series of mostly unfossiliferous formations composed mostly of sandstones (mainly continental) with intercalations of clays and shales which are commonly termed the Nubian Sandstone Series. These sediments vary in thickness from some few tens of meters in the northern regions of Sudan to about 4500 m in the northern part of the Kufra Basin (Klitzsch and Wycisk, 1999).

The lithostratigraphic units forming the body of the NSAS have a geologic age ranges from Cambro-Ordovician to Upper Cretaceous of continental origin with some marine intercalations of Devonian, Carboniferous and Turonian age (Bellini and Massa, 1980; Wycisk, 1987, 1993, 1994; Klitzsch, 1989; Said, 1990). To the north of the study area a great pile of marine sediments of Upper Cretaceous-Tertiary age is overlying the Sandstone Nubian sediments. Quaternary deposits are represented by fluvial deposits in the Nile Valley and Delta, gravel terraces bordering the Nile valley, lacustrine deposits covering the ground surface in some of the depressions, and Wadi fillings at the edges of the desert plateau and in the Eastern Desert (Fig. 2). Lake sediments and Sabkhas are major constituents of the surface of most of the depressions and oases, as they occur in thickness reaching 60 m in Sudan and the Kufra depression and about 40 m in the Kharga oasis (Kröpelin, 1999; Gossel et al., 2004).

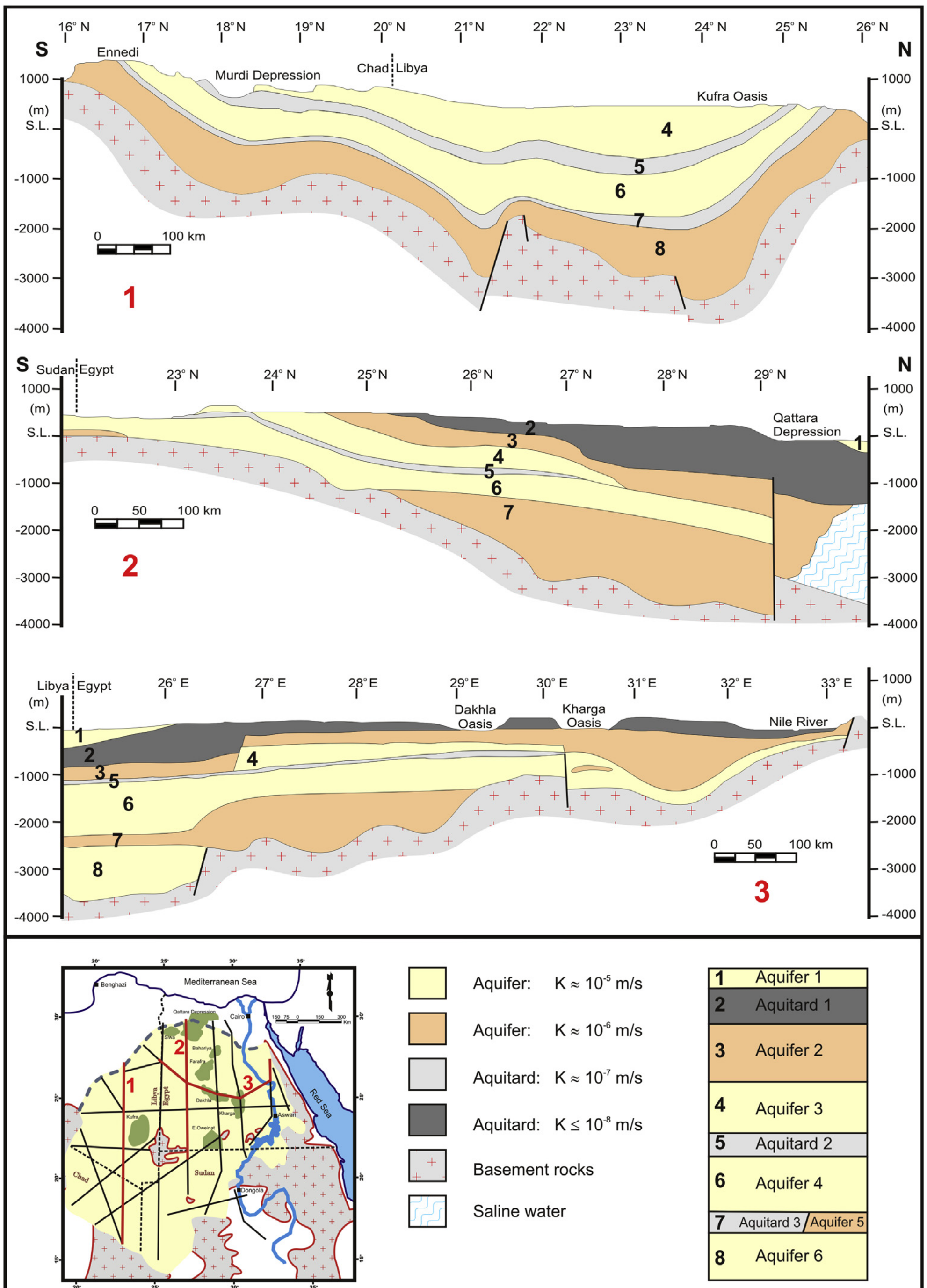

Fig. 3. Schematic example configures the conceptualization process and the location of some regional cross sections in plan view (Modified after Hesse et al., 1987).

Widespread free-moving sand deposits in the form of sand dunes and sand sheets are found on the top of a great part of the study area (Said, 1990).

Since early Paleozoic time vertical movements in this area have been very slow and are epeirogenesis in nature They led to the formation of the large basins of the area, which are now filled up with sediments over 4500 m thick and bordered or separated by zones of minor subsidence or uplift (Klitzsch, 1983; Schandelmeier et al., 1987; Wycisk et al., 1990).

Hydrogeologically, the NSAS is considered as a broadly closed system, as it has natural boundaries to the east and southeast formed by the mountain ranges of the Nubian Shield and is bounded to the south and west by the mountainous outcrops of Kordofan Block, Ennedi, and Tibesti. To the southwestern part of the basin, the aquifer is bounded by the groundwater divide located between Ennedi and Tibesti Mountains.

The natural northern boundary of the NSAS is set to the so-called Saline–Freshwater Interface, whose location is considered spatially stable, although slight movement is believable (Thorweihe and Heinl, 2000; Gossel et al., 2010a,b). The NSAS has a complex structure, which precludes adequate identification of the hydraulic continuity between the various sub-basins. The hydraulic interconnection is emphasized between sub-basins as well as between the different basins forming the system at the regional level (Sefelnasr, 2002, 2007; Gossel et al., 2008).

The hydraulic conductivities of the NSAS can also be introduced according to the lithologic components of every basin of the aquifer as in Fig. 3. The accuracy of these parameters depends on the locality and number of aquifer tests held; for instance, the Paleozoic layers are hardly penetrated by a well, so their parameters are always given as an average in correlation to the values calculated for the same layers in different localities, where they are partially or fully penetrated.

3. Material and methods

As a potential start with the groundwater flow modeling, a Geodatabase coherent structure has been built to accomplish a trustworthy and logical data set and to facilitate the further work. Several assumptions were considered in this study to describe the real aquifer system based on the understanding of the hydrogeology of the region for determining model boundaries, the number of aquifer layers to be modeled, and the location and extent of each aquifer layer. The number of the hydrostratigraphic units differs naturally from one location to another. Fig. 3 illustrates the typical cross sections showing the hydrostratigraphic interpretation of the lithologic, hydrogeologic, and borehole data. According to the hydrogeologic information, the aquifer was discretized vertically into eight hydrogeologic layers (five aquifers and three aquitards) as shown in Fig. 3.

These layers were further discretized numerically into three layers each to enhance the vertical distribution of the hydraulic conductivity to have a total of 22 numerical layers or 23 slices, this helped in reflecting the aquifer anisotropy as well. The aquifer parameters for the NSAS were carefully collected from the field observations given by national authorities (i.e. RIGW, 1999), as well as prior modeling publications for the NSAS (i.e. Ahmad, 1983; Sonntag, 1986; Hesse et al., 1987; Nour, 1996; Thorweihe and Heinl, 1999; CEDARE, 2002; Ebraheem et al., 2002; Sefelnasr, 2002; Bakhbakhi, 2006). The continental sandstone of Paleozoic to Cretaceous age was assigned to five different aquifers with hydraulic conductivities ranging fairly between 10^{-4} and 10^{-6} m/s. The lateral continuity of each aquifer within the different basins, as well as among these basins, is shown. The aquitards were assigned to have hydraulic conductivity values ranging from 10^{-7} to 10^{-9} m/s.

Because of the uneven distribution, quality, reliability, and the scarcity of the data sets from various sources, screening and data

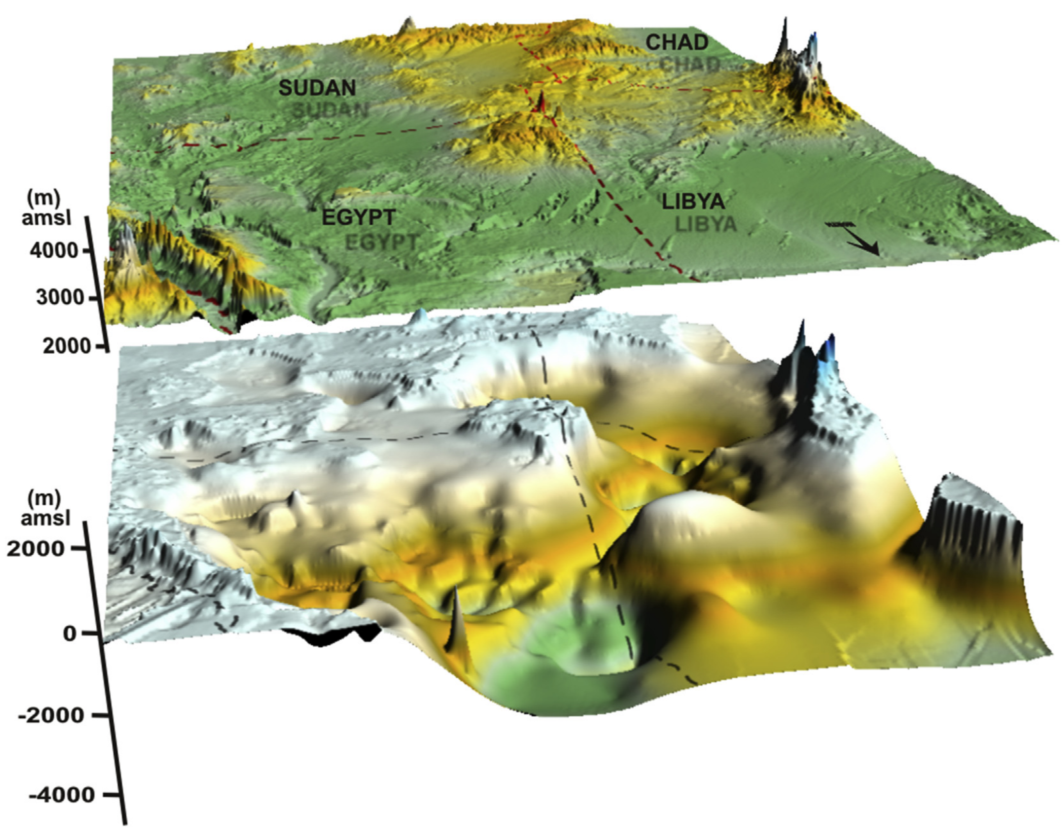

Fig. 4. Digital Elevation Model (DEM) and basement relief of the Nubian Sandstone Aquifer System.

Table 1
The different extraction scenarios (Mm^3/y) for the different stress areas within the NSAS.

Area	Scenario 1	Scenario 2	Scenario 3	Scenario 4	Scenario 5
Siwa	26	71	116	161	206
Bahariya	34	70	105.5	141	177
Farafra	283	330	377	424	471
Dakhla	439	485.5	532	578.5	625
Kharga	93	120.5	148	175.5	203
E. Oweinat	164	423	682	941	1200
Tushka	7.3	7.3	7.3	7.3	7.3
Kufra	183	685	1186.5	1688	2190
Tazerbo	126	189	252	315	378
Serir	73	110	146.5	183	220
Selima	102	102	102	102	102

Sources: MPWWR (1999), RIGW (1999), Pallas and Salem (2001), CEDARE (2002) and Bakhbakhi (2006).

quality control were essential in the development of the conceptual model, consequently the database. The interfaces between the different units and the hydraulic conductivity fields within each unit were defined on the basis of borehole data. To obtain laterally continuous layer elevations and hydraulic conductivities throughout the whole domain, the spot elevations and conductivities were interpolated using the appropriate geostatistical methods.

On account of this scarcity, discontinuity, and the scattered distribution of the data needed for the establishment of 3D groundwater flow model as intended in this work, a great effort was given to statistical management of the available data. The interpolation process was used to estimate, predict and fill gaps in the available datasets. The most known and representative statistical method is Kriging, which is a geostatistical regression gridding technique used to flexibly approximate or interpolate data. Kriging can be custom-fit to the datasets by specifying an appropriate variogram model, which is a three dimensional function used to match the spatial correlation, surfaces' roughness and continuity of the observed variables. The result was a grid composed of more than 2.7 million data points for each interpolated surface. These complex datasets become difficult to process due to data volume, variety, unknowns and uncertainties. Data management using GIS facilitated the process, validation, analysis, structuring, transformation and visualization of the data.

It was a crucial phase to approximate, analyze, understand, and graph the values of the data gaps and to plot an indiscrete, reasonable database for the NSAS. Since building surfaces separately does not ensure that they are consistent in the correct stratigraphic order, the GIS-techniques were used to control this process. In which spatial analysis, layers overlay, raster calculations, topology corrections, query, link to attribute tables, etc. were used. This helped in correcting errors such as crossovers raised from interpolation, checking thicknesses of layers and controlling the marginal range of the hydraulic parameters. The available records for the hydraulic conductivities were first imported into ArcGIS point data features, these subsequently were delogarithmized. The interpolation was held on the delogarithmized values of the hydraulic conductivities. At this step, a lot of constraint points had to be situated prior to the interpolation procedure to avoid problems of extrapolation.

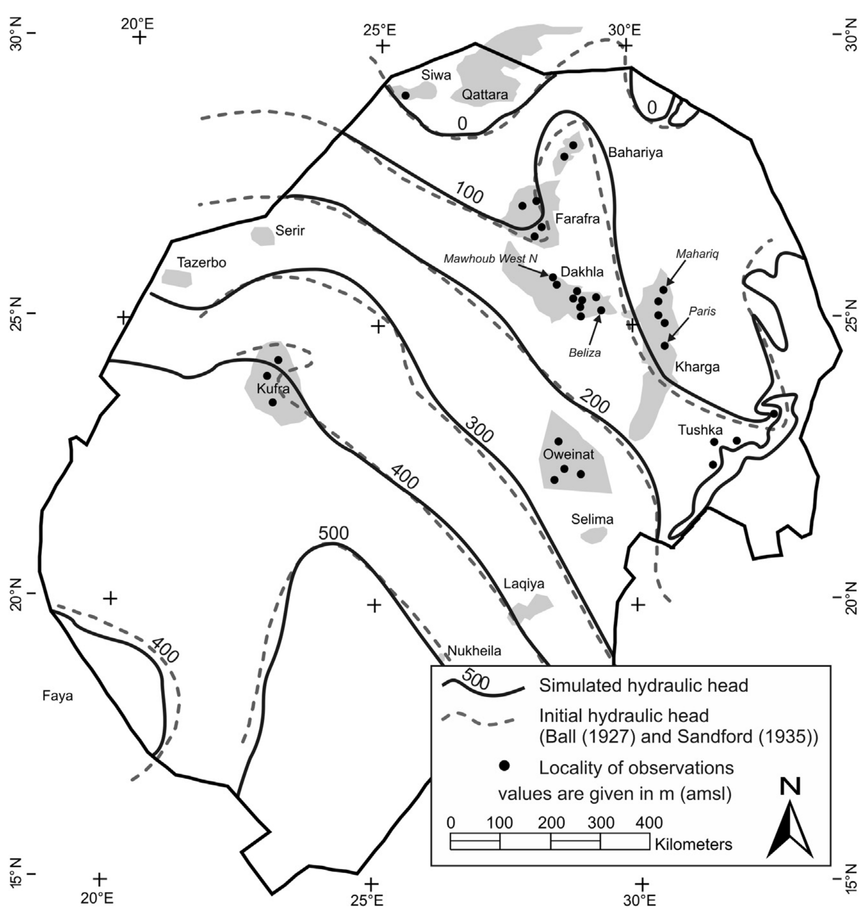

Fig. 5. The results of the calibration of the Nubian Sandstone Aquifer System.

Table 2
Calibration statistics for simulated hydraulic heads of the NSAS.

Calibration statistics	
Number of observations	928
Range of residuals (m)	23.97
Minimum residual (m)	−12.02
Maximum residual (m)	11.95
Mean residuals (m)	0.42
Standard deviation of residuals (m)	2.19
Root mean square residuals (m)	2.22
Calibration fit: standard deviation of residuals divided by average range of observed values	0.005

The first slice of the model structure was given from SRTM-03 (Shuttle Radar Topography Mission-03 Arc Seconds (Farr and Kobrick, 2000), about 90 m resolution). The other slices were generated originally from the available field data (cross sections, contour maps, topographic maps, well logs, etc.) as shown in Fig. 4.

4. Boundary conditions and calibration

A three-dimensional (3D) groundwater flow model for the NSAS was developed using the finite element modeling tool FEFLOW (Diersch, 2005). FEFLOW is a computational mesh that can incorporate complex geologic features; simulate rewetting/drying cells or saturated/unsaturated zone cases such as the NSAS. It has flexible mesh strategies that can develop and model unstructured grid refinements and solve large problems (>1 Million nodes) and allows for the modeling of three-dimensional (3D) groundwater flow problems and precise representation of the geometry and time dependent variables.

The whole aquifer domain is considered a closed system due to the natural boundaries consisting of the unfractured basement outcrops that bound the aquifer to the east, south as well as the west. In addition, the aquifer is bounded to the north by a hydrogeological boundary which is the Saline–Freshwater Interface. A fixed head boundary condition (Dirichlet 1st type boundary condition) was applied to the surface water body represented by Lake Nasser and to the Nile. A 2nd type boundary condition (Neuman) or flux boundary condition is represented in this modeling scheme by the “no flow boundary” that was set to the model outer boundaries due to the physical and hydrogeological boundaries.

The 4th type (Well boundary condition) of hydrogeological boundary condition is presented by the artificial discharge through pumping wells in the oases and development areas of the NSAS. Five extraction scenarios were suggested for the prediction simulation. The actual extraction rates were considered as scenario 1 and the planned extraction rates were assigned as scenario 5 as shown in Table 1. Three further scenarios were developed between these two major scenarios to evaluate the most reasonable extraction rates that do not result in uneconomic depths to groundwater. The model was first calibrated under the assumption of steady-state conditions.

The reference to this simulation was the groundwater contour maps of potentiometric levels for the aquifer of Ball (1927) and its modification that was presented by Sandford (1935). This map was chosen because it is the most reliable map representing the hydraulic head in the aquifer before the start of applying the artificial stresses on the aquifer in 1960 (Fig. 5).

The groundwater flow model of the NSAS was then calibrated and validated under transient conditions by use of the available historical hydraulic head records as calibration targets and was adjusted using a trial and error parameter estimation method through a series of groundwater flow simulations. The calibration process was designed for the period 1960–2005 (from the beginning of the New Valley Project until the last available field record) and a good calibration fit was obtained for this period.

The calibration was held by using the historical records of hydraulic head data of 56 wells. Measures of goodness-of-fit typically summarize the discrepancy between the simulated values and the observed ones. An accuracy analysis of water level data provides a calibration target of acceptable margin of error (Table 2). The residuals are assumed normally distributed over the 1:1 line of the scatter diagram as shown in Fig. 6. An evapotranspiration value of 10–15 mm/y was assigned to depressions of the study area (Himida, 1970; Ahmad, 1983; Sonntag, 1986; Sonntag and Christmann, 1987; Nour, 1996). This unbalanced loss from fossil groundwater storage induces an exponential decay of hydraulic head around the depressions, which is equivalent to a mean regional decline rate of the groundwater level of 0.5 cm/y as given by Sonntag (1986) and Thorweihe and Heinl (1999). As the area is extremely arid and subjected only to seasonal rains at the south, a recharge rate of 10–15 mm/y was applied to the simulation (Sonntag, 1986; Hesse et al., 1987; Thorweihe and Heinl, 1999;

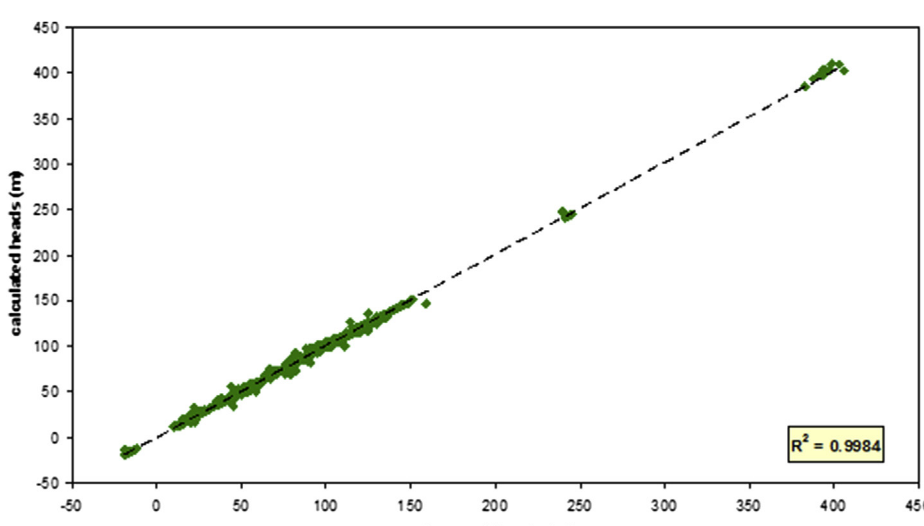

Fig. 6. Scatter diagram showing calculated vs. observed heads at calibration targets. The histogram represents the frequency range of the residuals.

Sonntag, 2001; CEDARE, 2002; Ebraheem et al., 2002; Gossel et al., 2004). Those values for evapotranspiration and recharge were calibrated by Ebraheem et al. (2002), Sefelnasr (2002) and Gossel et al. (2004). The evapotranspiration was also estimated in East Oweinat area, in the Western Desert of Egypt (Fig. 1) using the Thornthwaite method (Thornthwaite, 1948).

5. Simulation results and discussion

The ambitions for development in the Western Desert of Egypt and Kufra Oasis in Libya are great as can be seen from the official planned extraction rates from the NSAS (Table 1). Yet, these ambitions should be based on water availability, "sustainability" and socio-economic aspects along with water demand, not only the later. This work is a representation of how far/long the NSAS can afford artificial stresses without severe responses. Based on the actual (Scenario 1) and planned extraction rates (Scenario 5), scenario 2, 3, and 4 were obtained by increasing the rates of scenario 1 by 25%, 50%, and 75%, respectively, of the difference in rates needed to reach scenario 5. In the prediction simulation, the extraction rates for each scenario were assumed constant until year 2100. Climate conditions were assumed unchangeable in the prediction simulation. The Evapotranspiration was set to upper most surface and dependent on depth to groundwater, hence, it is adjusted to decrease as the depth to the groundwater increases.

The calibrated regional model was originally used to forecast the changes in the flow regime that result from the natural stresses and the anthropogenic activities on the aquifer resources during the coming 100 years. In the analysis procedure of the simulation results, emphasis was given to the changes in hydraulic head, drawdown, depth to groundwater, as well as the groundwater balance to evaluate the potential and response of the aquifer to the stresses above mentioned within the prediction period for each scenario.

In general, the direction of groundwater flow within the regional model area is kept by the original trend of the initial head as shown in calculated head in year 2005 (Fig. 7). However, the values and local trends of these contours showed some changes within the depressions like the Dakhla and Kharga oases and development areas like East Oweinat, where new closed contour

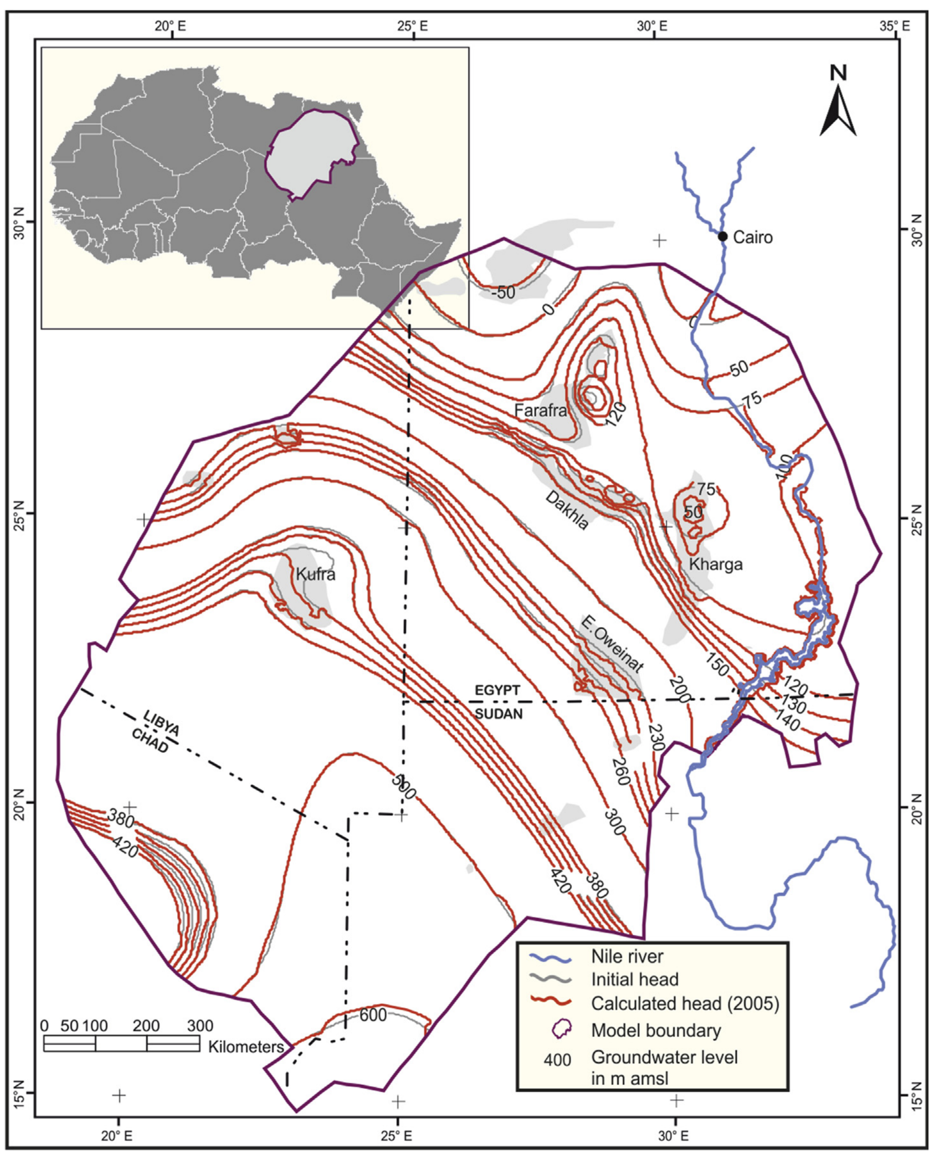

Fig. 7. The distribution of the simulated hydraulic head of the NSAS by 2005 in comparison to the initial heads of year 1960.

lines with lower values appeared. Before the project of the development of the New Valley has started, or rather before year 1960, there was no obvious drawdown within the studied depressions. Once the successive groundwater extraction was in progress, the amount of the groundwater stored in the aquifer started decreasing, leaving a noticeable decline in the potentiometric level as can seen after 45 years simulation time (2005) that represented by Fig. 8.

The results obtained from scenario 1 indicate that the major cones of depression are centered in the Kharga and Dakhla oases with average drawdown of 40 m and 42 m by 2050, respectively (Fig. 9a). This amount of decline in hydraulic head increases further for both oases to reach an average of 55 m by 2100. Nonetheless, the amounts mentioned above are an average drawdown, which does not hinder the existence of drawdown values that exceed 50 m by 2100 (Fig. 9b), for example, within the well fields of Kharga city in the Kharga oasis or east of the Dakhla oasis.

At the other depressions and the East Oweinat area, gentle cones of depression are formed without exposing anomalies of the hydraulic gradient or deepness of the cones of depression. However, with application of scenario 5, very steep hydraulic gradients and wide, deep cones of depression were created around the well fields by 2100 in Kharga, Dakhla, and East Oweinat in Egypt; Kufra, Serir, and Tazerbo in Libya; and Laqiya in Sudan (Fig. 9c).

The cones of depression around Dakhla, Farafra, and Bahariya are extended to build a huge single cone of depression gathering the whole area occupied by the three oases. The two meter drawdown line is located about 145 km south of the well fields of the Dakhla oasis. In the East Oweinat area, the cone of depression extends to the south beyond the state boundary between Egypt and Sudan to form a very deep cone of depression with an average value of 162 m and a maximum value exceeding 200 m at several locations by year 2100 (Fig. 9c).

The same situation of East Oweinat area was found in Kufra oasis, where maximum drawdown that exceeding 200 m was also recorded. The optimization process of the model for East Oweinat area and Kufra oasis in terms of the abstraction rates shows that scenario 3 is the best option for the groundwater management. The average depth to groundwater by 2100 will not exceed 90 m and 85 m for Kufra and East Oweinat, respectively, in this scenario. So it is concluded that scenario 3 is economically the optimal development scenario at these areas as shown in Fig. 9d.

The uncertainties in the predicted drawdown for the NSAS were quantified and described using the mean and standard deviation (SD) as presented in Table 3. The mean portrays the central tendency or average drawdown and the standard deviation characterizes the variability in drawdown about the central tendency. The standard deviation is factor that considered as a boundary for the

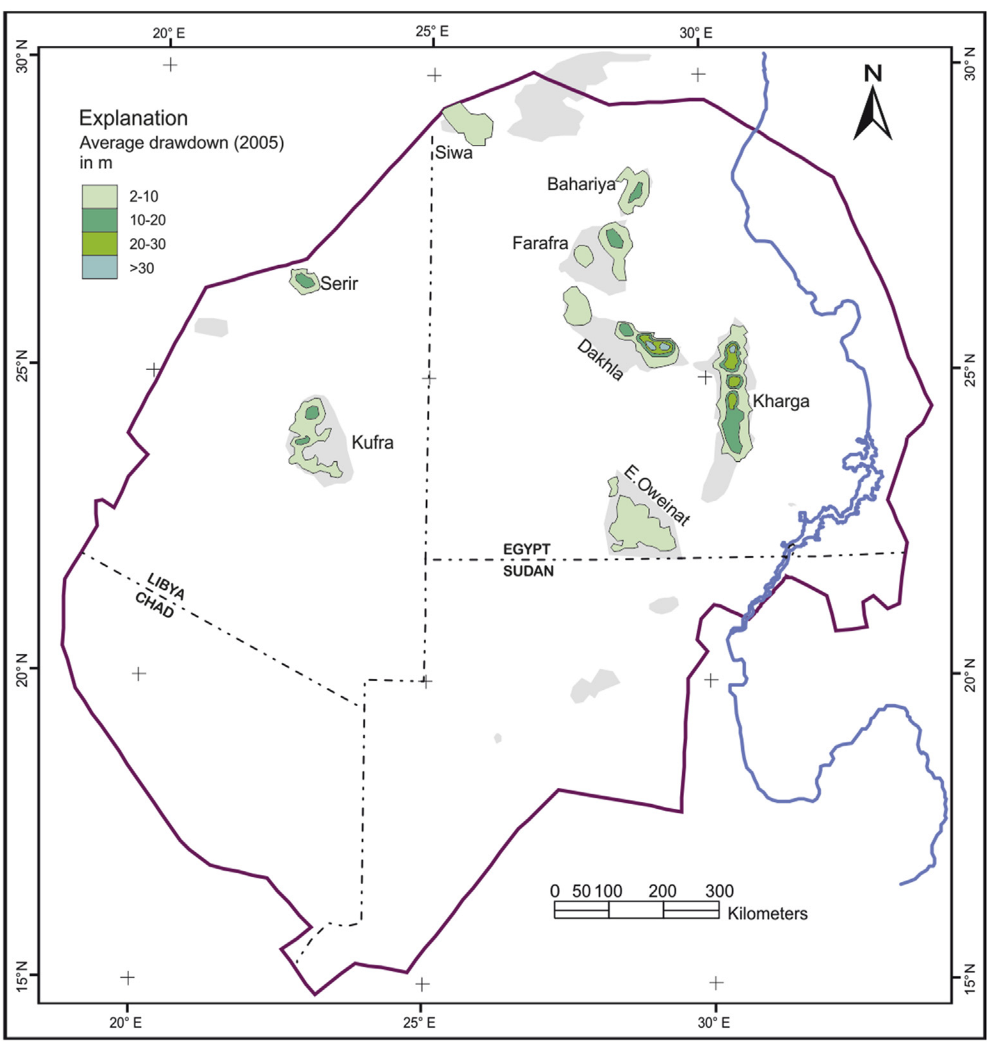

Fig. 8. The drawdown within the depressions of the NSAS by 2005.

predicted results. The standard deviation increases with time indicating that uncertainty in drawdown increases over time (Table 3).

A groundwater balance for the NSAS for the period 1960–2100 was calculated to obtain a more detailed picture of the behavior of the aquifer system to the different anthropogenic activities. It can be concluded that the annual change in storage is typically contingent on the changes of the extraction rates. For scenario 1 (Fig. 10) the extraction rate decreases gently to reach about −0.5 km^3 by 1980. In the same case the annual change in storage reaches about 0.3 km^3 after a little swaying from positive to negative values at the very beginning of the simulation. The parallelism between these two components indicates that every additional extraction is groundwater mining. It is also concluded that during the period from 1960 to 2005, the total artificial discharge by pumping increased from 0.16 km^3/y to 1.8 km^3/y,

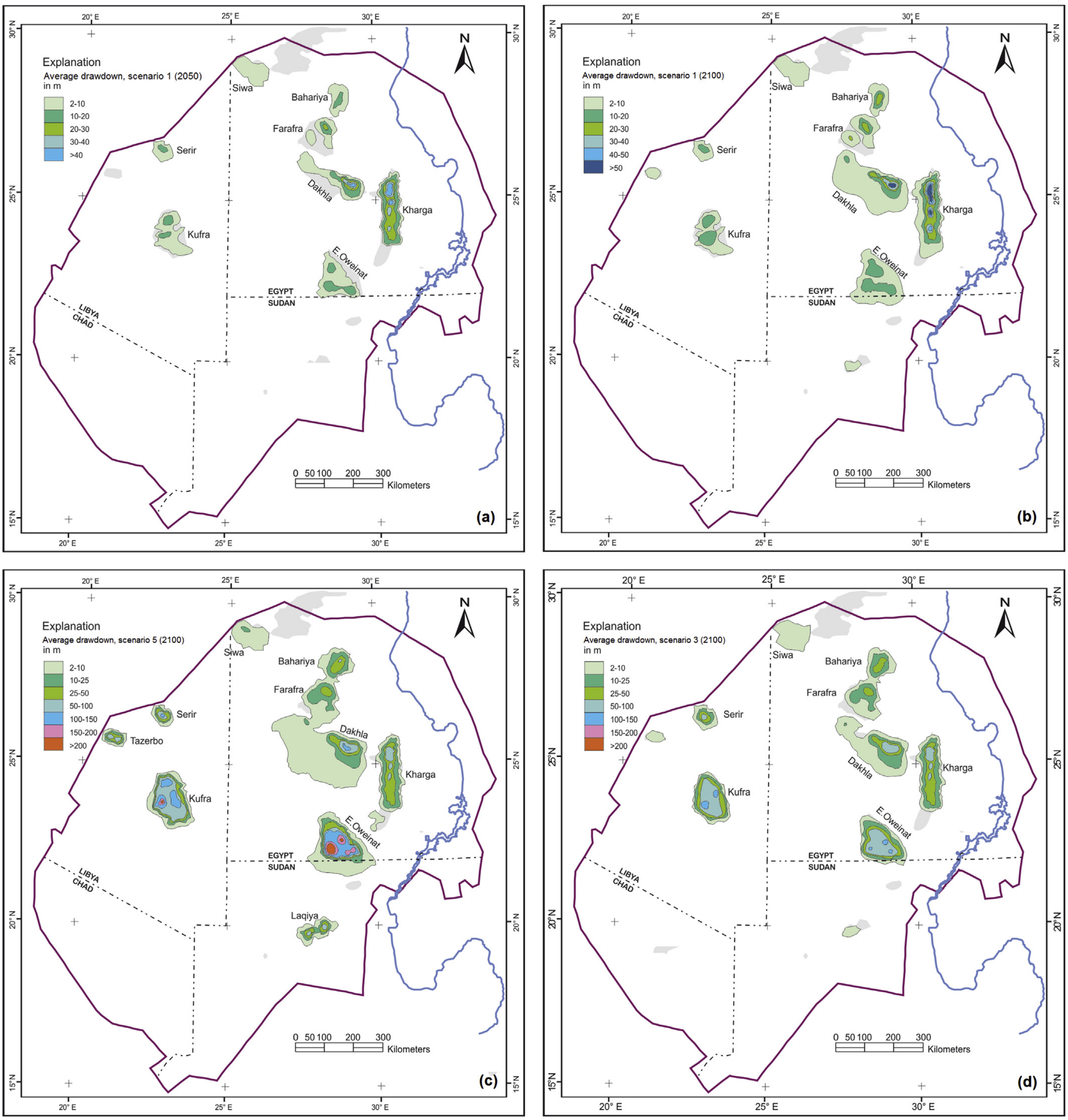

Fig. 9. (a): Resulting drawdown by 2050 in the NSAS, suggesting the extraction rates of scenario 1 are constant until 2100, (b): Resulting drawdown by 2100 in the NSAS, suggesting the extraction rates of scenario 1 are constant until 2100, (c): Resulting drawdown by 2100 in the NSAS, suggesting the extraction rates of scenario 5 are constant until 2100, (d): Resulting drawdown by 2100 in the NSAS, suggesting the extraction rates of scenario 3 are constant until 2100.

Table 3
Drawdown uncertainties quantification for different scenarios and locations within the NSAS for years, 2005, 2050 and 2100.

Metrics			Dakhla			Kharga			Farafra			Bahariya			Siwa			E. Oweinat			Kufra		
			2005	2050	2100	2005	2050	2100	2005	2050	2100	2005	2050	2100	2005	2050	2100	2005	2050	2100	2005	2050	2100
Mean (m)	Scenario	1	25	42	55	30	40	55	8	20	33	7	16	22	6	10	15	5	11	18	7	11	16
		2	25	49	68	30	40	55	8	23	40	7	21	31	6	12	18	5	44	77	7	39	71
		3	25	60	85	30	40	55	8	30	55	7	28	47	6	17	24	5	80	145	7	70	130
SD (m)	Scenario	1	5.5	16.2	22.1	8.1	14.6	25.3	1.7	6.8	15.9	1.2	6.7	10.3	1.3	2.6	7.1	1.1	5.9	8.4	2.1	4.4	7.7
		2	5.5	18.6	28.9	8.1	14.6	25.3	1.7	10.6	19.3	1.2	9.9	15.1	1.3	4.6	7.6	1.1	20.5	36.8	2.1	18.6	34.5
		3	5.5	28.3	23.1	8.1	14.6	25.3	1.7	13.9	24.6	1.2	14.6	22.3	1.3	6.9	1.7	1.1	38.6	75.8	2.1	33.1	66.3

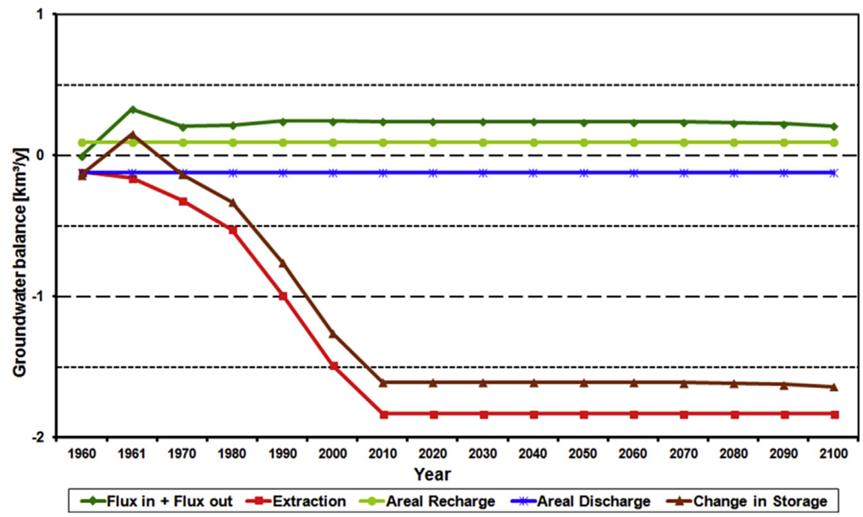

Fig. 10. Groundwater balance for the NSAS for the period 1960–2100, scenario 1.

while inflow stayed still almost the same in case if the actual extraction rates are still constant until 2100.

6. Conclusion

A 3D groundwater flow model for the NSAS was developed and calibrated. This model is based on the concept that the NSAS is replenished and was never under steady state as given by many authors (i.e. Ebraheem et al., 2002; CEDARE, 2002; Gossel et al., 2004). This model was designed to have horizontal spatial discretization as small as 100 m where the stresses and boundaries are to be applied. This gave it an advantage with comparison to other regional models (with best resolution of 10 km) that it can accurately represent the hydraulic parameters, precisely reflect the curvature of head and hydraulic gradient, properly define the boundaries and exactly locate the pumping wells and stresses.

The modeled geometric volume is about 3.5×10^6 km^3 and the calculated groundwater volume is about 212×10^3 km^3. Thorweihe and Heinl (2002) estimated the groundwater volume of NSAS at 150,000 km^3, and CEDARE (2002) estimated the fresh groundwater volume at 372,950 km^3. However, the modeled area by CEDARE (2002) was extended to the Mediterranean coast in the north.

A great effort was given to the development of a coherent, reliable conceptual model for the NSAS to mimic the real world as close as possible, this step based on constructing a geodatabase that is advantageous of being updatable and easily linkable to the modeling systems. The simulation indicated that the potentiometric level was still above ground level in many oases, which means that the extraction wells were still under free flowing conditions. The simulation of the actual extraction rates indicated that by 2100 the average drawdown in the Dakhla and the Kharga oasis will be about 55 m and, while in the Kufra oasis and the East Oweinat area the average drawdown will not exceed 16 and 18 m, respectively.

At the end of the simulation the free flowing phenomenon will disappear all over the modeled area and the average depth to groundwater will range from 5 m (bgl) in the Bahariya oasis to 36 m in the Kharga oasis. In 2100 a groundwater volume of 354 km^3 will be extracted from the aquifer storage. The simulation of the planned extraction rates resulted in average decline in hydraulic head by 2100 over 130 m in the Kufra oasis and the East Oweinat area. The average depth to groundwater will increase successively during the simulation to overtake the limit of 100-m (bgl) of the economic lifting depth in the Kufra oasis and the East Oweinat area by 2100. This, in turn, will lead to unfavorable environmental impacts within the development areas. This conclusion was also given by Sefelnasr et al. (2014) and Voss and Soliman (2014). Although the size of the cones of depression remarkably increase over time, they traverse the political boundaries only south of East Oweinat to area towards Sudan and west of Siwa oasis.

The phenomenon of the free flowing wells will disappear from the entire domain by 2030. The groundwater volume extracted from the aquifer storage until 2100 exceeds roughly 1400 km^3. Based on the groundwater availability and demand, the proposed economic lifting depth, and the development ambitions for the NSAS, the application of the extraction rates of scenario 3 was found to be the best management option that meets these topics. As by 2100 the average depth to groundwater will not exceed 90 m and 85 m (bgl) in the Kufra and the East Oweinat, respectively, where the highest extraction rates were applied. The groundwater management of the NSAS should be based on the “aquifer depletion concept", as the groundwater extraction from this aquifer is a groundwater mining.

Appendix A. Supplementary data

Supplementary data related to this article can be found at http://dx.doi.org/10.1016/j.jaridenv.2015.06.009.

References

Ahmad, M.U., 1983. A quantitative model to predict a safe yield for well fields in Kufra and Sarir basins, Libya. Ground Water 21 (1), 58–66.

Bakhbakhi, M., 2006. Nubian Sandstone Aquifer System. IHP-VI-series on Groundwater. UNESCO, Paris, pp. 75–81. No 10.

Ball, J., 1927. Problems of the Libyan Desert. Geogr. J. 70 (21–38), 105–128, 209–224.

Bellini, E., Massa, D., 1980. A stratigraphic contribution to the Paleozoic of the southern basins of Libya. In: Salem, M.J., Brusrewi, M.T. (Eds.), The Geology of Libya. Elsevier, Amsterdam, pp. 1–289.

CEDARE, 2001. Regional Strategy for the Utilization of the Nubian Sandstone Aquifer System. In: Hydrogeology, vol. II. Centre for the Environment and Development for the Arab Region and Europe, Cairo, Egypt.

CEDARE, 2002. Regional Strategy for the Utilization of the Nubian Sandstone Aquifer System. Draft final report. Centre for Environment and Development for the Arab Region and Europe, Heliopolis Bahry, Cairo, Egypt, pp. 22–82.

Cloudsley-Thompson, J.L., 1984. Sahara Desert. Perhamon Press, Oxford, p. 384.

Conoco, 1987. Geologic Map of Egypt, 20 Sheets, Scale 1:500 000. Egyptian General Authority for Petroleum (UNESCO, Joint Map Project), Cairo, Egypt.

Diersch, H.J., 2005. FEFLOW, Finite Element Subsurface Flow and Transport Simulation System, Reference Manual. Wasy Institute for Water Resources Planning and Systems Research Ltd, Berlin, Germany, p. 292.

Ebraheem, A., Riad, S., Wycisk, P., Seif El-Nasr, A., 2002. Simulation of impact of present and future groundwater extraction from the non-replenished Nubian sandstone aquifer in southwest Egypt. Environ. Geol. 43 (1–2), 188–196.

Ebraheem, A., 2003. A large-scale groundwater flow model for the New Valley area with a telescoping mesh on Kharga oasis, SW Egypt. Jahrb. für Geol. Paläontol. Abh 228, 153–174.

Ebraheem, A., Garamoon, H., Riad, S., Wycisk, P., Seif El-Nasr, A., 2003. Numerical modeling of groundwater resource management options in the East Oweinat area, SW Egypt. Environ. Geol. 44 (4), 433–447.

Ebraheem, A., Riad, S., Wycisk, P., Sefelnasr, A., 2004. A local-scale groundwater flow model for modeling ground-water resources management options in Dakhla Oasis, SW Egypt. Hydrogeol. J. 12 (6), 714–722.

El-Baz, F., Maingue, M., Robinson, C., 2000. Fluvio-aeolian dynamics in the northeastern Sahara: the relationship between fluvial/aeolian systems and groundwater concentration. J. Arid Environ. 44 (2), 173–183.

Farr, T.G., Kobrick, M., 2000. Shuttle radar topography mission produces a wealth of data. Amer. Geophys. Union Eos 81, 583–585.

Ghoneim, E., El-Baz, F., 2007. The application of radar topographic data to mapping of a mega-paleodrainage in the Eastern Sahara. J. Arid Environ. 69 (4), 658–675.

Gossel, W., Ebraheem, A.M., Wycisk, P., 2004. A very large scale GIS-based groundwater flow model for the Nubian sandstone aquifer in Eastern Sahara (Egypt, northern Sudan and eastern Libya). Hydrogeol. J. 12 (6), 698–713.

Gossel, W., Sefelnasr, A., Ebraheem, A., Wycisk, P., 2006. Large scale recharge modeling in the arid area of the eastern Sahara. In: Recharge Systems for Protecting and Enhancing Groundwater Resources. Proceedings of the 5th International Symposium on Management of Aquifer Recharge (ISMAR5), Berlin, Germany, IHP-VI, Series on Groundwater No 13, pp. 877–882.

Gossel, W., Sefelnasr, A., Ebraheem, A., Wycisk, P., 2008. A GIS-based flow model for groundwater resources management in the development areas in the eastern Sahara, Africa. No 13. In: Adelana, S.M.A., MacDonald, A.M. (Eds.), Applied Groundwater Studies in Africa. IAH Selected Papers on Hydrogeology. CRCPress/Balkema, Leiden, The Netherlands, pp. 43–64.

Gossel, W., Sefelnasr, A., Weise, S.M., Friese, K., Stefanova, A., Wycisk, P., 2010a. Hydrochemical and isotope analysis of deep groundwater from the Nubian Aquifer System in the Egyptian Oases. In: XXXVIII IAH Congress, Abstract Book (Groundwater Quality Sustainability), Krakow 1–2, p. 519.

Gossel, W., Sefelnasr, A., Wycisk, P., 2010b. Long term modeling of saltwater intrusion in the northern part of the Nubian Aquifer System. Hydrogeol. J. 18 (6), 1447–1463.

Heinl, M., Brinkmann, P.J., 1989. A ground water model for the Nubian Aquifer System. IAHS, Hydrolog. Sci. J. 34 (4), 425–447.

Hermina, M., 1990. The surroundings of Kharga, Dakhla and Farafra oases. In: Said, R. (Ed.), The Geology of Egypt. Balkema, Rotterdam, pp. 259–292.

Hesse, K.H., Hissene, A., Kheir, O., Schnaecker, E., Schneider, M., Thorweihe, U., 1987. Hydrogeological investigations of the Nubian Aquifer System, Eastern Sahara. Berl. Geowiss. Abh. (A) 75, 397–464.

Himida, I.H., 1970. The Nubian artesian basin, its regional hydrogeological aspects and palaeohydrological reconstruction. J. Hydrol. 9, 89–116.

Ibrahim, M.M., 1956. The origin of the depressions in the Libyan Desert. Obs. Proc. Geol. Soc. Egypt 2 (1), 6–20.

Klitzsch, E., 1983. Geological research in and around Nubia. Episodes 3, 15–19.

Klitzsch, E., 1989. Zur Stratigraphie Nubiens. Z. Dt. Geol. Ges. 140, 151–160.

Klitzsch, E., Wycisk, P., 1999. Beckenentwicklung und Sedimentations prozesse in Kratonalen Bereichen Nordost-Afrikas im Phanerozoikum. In: Klitzsch, E., Thorweihe, U. (Eds.), Nordost-Afrika: Strukturen und Ressourcen. John Wiley & Sons-VCH, Weinheim, pp. 61–108.

Knetsch, G., Yallouze, M., 1955. Remarks on the origin of the Egyptian oases depressions. Bull. Soc. Geogr. Egypt 28, 21–33.

Kröpelin, S., 1999. Terrestrische Paläoklimatologie heute arider Gebiete: resultate aus dem Unteren Wadi Howar (Südöstliche Sahara/NW-Sudan). In: Klitzsch, E., Thorweihe, U. (Eds.), Nordost-Afrika: Strukturen und Ressourcen. John Wiley & Sons-VCH, Weinheim, pp. 448–508.

Kröpelin, S., 2001. Inter-hemispheric correlation of monsoon controlled climatic change in Northeast Africa with climate evolution in southwest Africa during the past 20,000 years. Geophys. Res. Abstr. 3, 317–323.

MPWWR, 1999. Groundwater Development and Management Strategies for the New Valley. Ministry of Public Works and Water Resources Internal report, Cairo, pp. 11–22.

NASA, 2005. Shuttle Radar Topography Mission Data Sets. National Aeronautics and Space Administration. http://www.jpl.nasa.gov/srtm (accessed April 2007).

NASA, 2006. Visible Earth, a Catalog of NASA Images and Animations of Our Home Planet. National Aeronautics and Space Administration. http://visibleearth.nasa.gov (accessed April 2013).

Nour, S., 1996. Groundwater potential for irrigation in the East-Oweinat area, Western Desert, Egypt. Environ. Geol. 27, 143–154.

Pachur, H.J., Roepr, H.S., Kroepelin, S., Goschin, M., 1987. Late Quaternary hydrography of the Eastern Sahara. Berl. Geowiss. Abh. (A) 75 (2), 331–384.

Pachur, H.J., Kröpelin, S., Hoelzman, P., Goschin, M., Altman, N., 1990. Late Quaternary fluvio-lacustrine environments of western Nubia. In: Klitsch, E., Said, R., Schrank, E. (Eds.), Results of the Special Research Project Geoscientific Problems in Arid and Semiarid Areas, Period 1987–1990. Berl. Geowiss. Abh. (A) 120 (1), 203–260.

Pachur, H.J., 1999. Paläo-Environment und Drainagesysteme der Ostsahara im Spätpleistozän und Holozän. In: Klitzsch, E., Thorweihe, U. (Eds.), Nordost-Afrika: Strukturen und Ressourcen. John Wiley & Sons -VCH verlag GmbH, Weinhaim, pp. 366–445.

Pallas, P., Salem, O., 2001. Water Resources Utilization and Management of the Socialist People Arab Jamahiriya. IHP-V, Technical Documents in Hydrogeology. UNESCO, Paris, pp. 147–172. No 42.

RIGW, 1999. A Plan for the Development and Management of Deep Groundwater in the Oases. Internal Strategy report. Research Institute for Ground Water, Cairo, p. 86.

Sadek, M.A., Abd El-Samie, S.G., El-Arabi, N.E., Ahmed, M.A., 2001. Hydrochemical, isotopic and age characteristics of the groundwater in the Nubian sandstone aquifer, South Western Desert, Egypt. Isot. Rad. Res. 33, 161–177.

Said, R., 1990. Geomorphology. In: Said, R. (Ed.), The Geology of Egypt. Balkema, Rotterdam, pp. 9–25.

Sandford, K.S., 1935. Geological observations on the southwestern frontiers of the Anglo-Egyptian Sudan and the adjoining part of the southern Libyan Desert. Q. Geol. Soc. Lond. 80, 323–381.

Schandelmeier, H., Klitzsch, E., Hendriks, F., Wycisk, P., 1987. Structural development of north-east Africa since Precambrian times, Berl. Geowiss. Abh. (A) 71 (1), 25–48.

Sefelnasr, A., 2002. Hydrogeological Studies on Some Areas in the New Valley Governorate, Egypt. Assiut University, Egypt (M.Sc. thesis).

Sefelnasr, A., Gossel, W., Wycisk, P., 2006a. GIS-based groundwater flow modeling of the Eastern Sahara. In: 8th International Conference on the Geology of the Arab World, Cairo, Egypt, pp. 194–195.

Sefelnasr, A., Gossel, W., Wycisk, P., 2006b. GIS-basierte Grundwasserströmungsmodellierung des Nubischen Aquifersystems, Westliche Wüste, Ägypten, vol. 43. SDGG – Schriftenreihe der Deutschen Gesellschaft für Geowissenschaften, DGG, Cottbus Heft, p. 161.

Sefelnasr, A., 2007. Development of Groundwater Flow Model for Water Resources Management in the Development Areas of the Western Desert, Egypt (DSc. thesis). Martin Luther University, Germany.

Sefelnasr, A., 2008. GIS-based Groundwater Flow Modeling. VDM Verlag Dr. Mueller, Saarbruecken, p. 171.

Sefelnasr, A., Gossel, W., Wycisk, P., 2014. Three-dimentional groundwater flow modeling approach for the groundwater management options for the Dakhla oasis, Western Desert, Egypt. Environ. Earth Sci. 72 (4), 1227–1241.

Sonntag, C., 1986. A time dependent groundwater model for the Eastern Sahara. Berl. Geowiss. Abh. (A) 72, 124–134.

Sonntag, C., Christmann, D., 1987. Groundwater evaporation from east Saharian depressions by measuring deuterium and oxygen-18 in soil moisture. Berl. Geowiss. Abh. (A) 75 (2), 385–396.

Sonntag, C., 2001. Assessment Methodologies: Isotopes and Noble Gases in Saharan Palaeowaters and Change of Groundwater Flow Pattern in the Past. IHP-VI, Technical Documents in Hydrogeology, vol. 42. UNESCO/IHP, pp. 205–220.

Sturchio, N.C., Du, X., Purtschert, R., Lehmann, B.E., Sultan, M., Patterson, L.J., Lu, Z.T., Müller, P., Bigler, K., O'Connor, T.P., Young, L., Lorenzo, R., Becker, R., El Alfy, Z., El Kaliouby, B., Dawood, Y., Abdallah, A.M.A., 2004. One million year old groundwater in the Sahara revealed by krypton-81 and chlorine-36. Geophys. Res. Lett. 31, L05503.

Thornthwaite, C.W., 1948. An approach towards a rational classification of climate. Geogr. Rev. 38 (1), 55–94.

Thorweihe, U., Heinl, M., 1999. Groundwater Resources of the Nubian Aquifer System. IHP V, Technical Documents in Hydrology, vol. 42. UNESCO, p. 23.

Thorweihe, U., Heinl, M., 2000. Map Hydrogeology of the Nubian Aquifer System. Scale 1:2,500,000.

Thorweihe, U., Heinl, M., 2002. Groundwater Resources of the Nubian Aquifer System, NE-Africa. Modified synthesis submitted to: Observatoire du Sahara et du Sahel. OSS, Paris, p. 23.

USGS-GEO-DATA, 2004. Geologic Data and Hazards of the World. United Stated Geological Survey, Geological Division, Geological Data, Reston, USA. http://geode.usgs.gov (accessed March 2013).

Voss, I., Soliman, S.M., 2014. The transboundary non-renewable Nubian Aquifer System of Chad, Egypt, Libya and Sudan: classical groundwater questions and parsimonious hydrogeologic analysis and modeling. Hydrogeol. J. 22, 441–468.

White, F., 1983. The Vegetation of Africa: a Descriptive Memoir to Accompany the UNESCO/AETFAT/UNSO Vegetation Map of Africa. UNESCO, Paris, p. 356.

Williams, M., Faure, H., 1980. The Sahara and the Nile. Balkema, Rotterdam, p. 622.

Wycisk, P., 1987. Contributions to the subsurface geology of the Misaha trough and the southern Dakhla basin (S. Egypt/N. Sudan). Berl. Geowiss. Abh. (A) 75, 137–150.

Wycisk, P., 1993. Outline of the geology and mineral resources of the southern Dakhla Basin, southwest Egypt. In: Meissner, B., Wycisk, P. (Eds.), Geopotential and Ecology: Analysis of a Desert Region. Catena Supplement, vol. 26, pp. 67–89.

Wycisk, P., 1994. Correlation of the major late Jurassic-early tertiary low- and high stand cycles of SW Egypt and NW Sudan. Geol. Rsch 83, 759–772.

Wycisk, P., Klitzsch, E., Jas, C., Reynolds, O., 1990. Intracratonal sequence development and structural control of Phanerozoic strata in Sudan. Berl. Geowiss. Abh. (A) 120, 45–86.